SOLDER PASTE: FUNDAMENTAL MATERIAL PROPERTY / SMT PERFORMANCE CORRELATION

Nilesh Badwe, Shunfeng Cheng, Srinivasa Aravamudhan, Mukul Renavikar
Intel Corporation
Hillsboro, OR, USA
nilesh.u.badwe@intel.com

ABSTRACT

Aggressive form factors, reducing pitch, thinner packages, and larger die to package ratios are leading to higher package warpage during SMT reflow. It is getting more challenging to mitigate warpage driven SMT defects viz. non-wet open (NWO), head-on-pillow (HoP) and solder bridging (SB). We studied multiple paste formulations using SMT hammer tests. Lab level characterizations were also used to establish a correlation between SMT performance and fundamental properties ofsolder pastes. We found that NWO and HoP compete with each other while having a correlation with flux activity to clean OSP on the Cu surface. SB risk showed a correlation with high temperature viscosity, indicating a rheology driven defect. Printability performance also showed a good correlation with the thixotropic index. These learnings will be extremely useful to develop next generation solder pastes to mitigate warpage driven defects.

Key words: Solder paste, SMT defects, Non-wet open, Head on pillow, Solder bridging, Structure-property correlation, Activity, Rheology.

INTRODUCTION

The Semiconductor industry is currently pushing the limits of Moore's law by packing increasing quantities of transistors on a chip. This leads to more aggressive requirements for the packaging technology in terms of geometric form factors such as thinner packages, thinner dies, larger die to package ratios, and smaller termination pitch. For Flip Chip Ball Grid Array (FCBGA) packages, all these trends result in a significant increase in the package warpage during SMT reflow soldering owing to the coefficient of thermal expansion (CTE) mismatch between the Si die and the package substrate. This high warpage during SMT reflow leads to multiple defects at the second level interconnect (SLI) solder joints. These defects include non-wet open (NWO), Head-on-Pillow (HoP) and Solder bridging (SB). As the package heats up during the SMT reflow process to a temperature of 250°C for typical Sn-Ag-Cu (SAC) based solder compositions, the package warpage level increases significantly. This leads to the package solder ball moving away from the solder paste deposit on the printed circuit board (PCB) pad in certain regions of the ball array, and the solder ball being compressed on the PCB pad in other areas. The SAC based solders melt at ~217-220˚C depending on Ag and Cu content. If the package is significantly warped while the solder is molten, compressive regions end up with solder bridging defects. If the BGA solder balls are in contact with the solder paste printed on the pads on the PCB, there is a likelihood of the paste sticking to the BGA ball while the package moves away from the PCB during reflow. This can result in the formation of non-wet open defects as shown in the Figure 1. Amir et. al. [1] found a measure of activity through wetting time and tackiness of the solder paste to have an impact on the NWO resistance using a limited number (3) of solder pastes. If the solder paste doesn't stick to the BGA solder ball and the ball moves away from the solder paste printed on the pad, flux from the solder paste won't be able to clean oxide on the BGA surface to form a joint between the solder from paste and the BGA leading to HoP type defects as also shown in the Figure 1. Amir et al. [2] found a correlation with viscosity and pH stability of the pastes with HoP risk. However, this study was limited to only 2 pastes. Amir also found that the solder balling rate correlates with the incidences of HoP defects, which points to a flux activity driven mechanism for creation of this defect.

For the compressed region under the package, flux flows out from the pads during the initial temperature ramp up stage of the reflow process and sometimes merges with the flux flowing out from an adjacent pad. This flux flow, prior to the solder paste melting, provides a path for the molten solder to bridge once the reflow temperature passes the melting temperature of the solder as shown in the Figure 1.

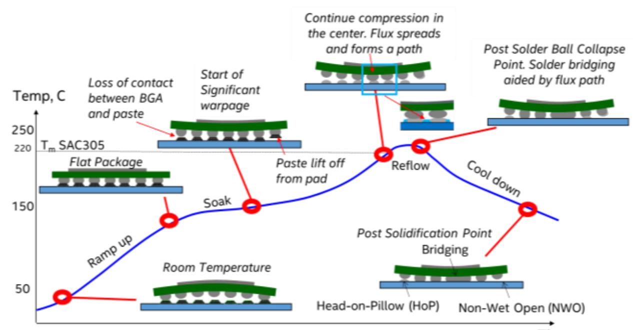

Figure 1: Warpage driven defect generation mechanism

All of these potential warpage-driven SMT defects can be avoided by changing the volume of paste printed on the PCB pads in regions within the pad array which are at a particularly high risk. Reduction in the stencil aperture in regions with high solder bridging risk can help reduce the solder bridging defects by reducing the volume of solder paste printed on the PCB pads. An increase in the paste volume through a larger stencil aperture will help keep the paste in continuous contact with the BGA and pad during SMT reflow. This helps eliminate NWO and HoP defects in regions within the ball area where the package substrate warps up from the PCB during reflow soldering. Such hybrid stencil aperture designs, as shown in the Figure 2, can help eliminate most defects. Pad design can also help to reduce SB risk. For example, Figure 3 shows two designs at the same pin location. It is easier to form flux/solder paths for the design (a) whereas the design (b) has room to keep flux around the pad, thereby avoiding flux bridging during the ramp up period and consequently solder bridging post reflow

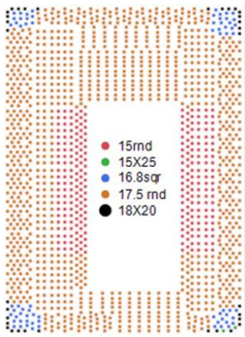

Figure 2. Multiple Aperture Sizes for a BGA (center is 15 mil circle, while corner is up to 18X20 rectangular

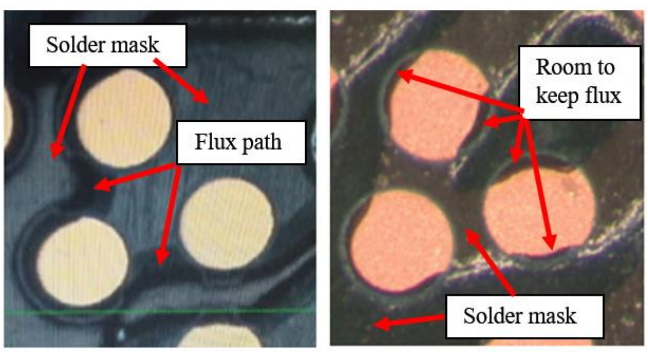

(a) Flux is easy to form paths. SBs observed

(b) Flux is limited around the pad. No SBs.

Figure 3. Pad design impacts availability of flux between solder pads to provide a path for solder to bridge

The optimization shown in Figure 3 above is able to eliminate most of the warpage driven defects. However, some packages still show excessive warpage outside of the typical range for a particular BGA product. Figure 4 shows counter plots of two packages from the same FCBGA product design. A majority of packages of that product have corner-up high temperature warpage as shown in Figure 4 (a), where the red color signifies that area is bending up above the plane of the paper. However, some packages show corner-down warpage as Figure 4 (b), where the blue color signifies the area bending down into the plane of the paper. Creating a uniform stencil design to fit both warpage conditions is difficult. If the stencil is designed based on a corner-up warpage shape, more paste will be delivered to corner pins and less paste in the center. This might lead to NWO and HoP defects in the center and solder bridging in the corner of the package. A paste which is more resistant to these defects would provide extra margin in such cases to minimize defects, thereby improving the SMT yield.

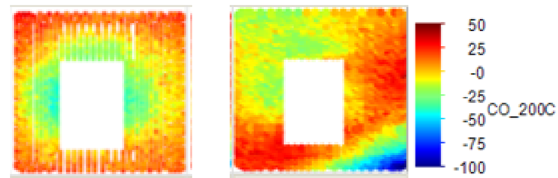

(a) Normal corner-up warpage

(b) Right corner down warpage

Figure 4. Two different packages from same lot with significantly different warpage profile at high temperature (200ºC). The scale bar shows warpage numbers in um.

In the current study, multiple solder pastes were evaluated using `SMT hammer tests` specifically designed to force the formation of each defect type. The fundamental properties of these pastes were also determined using lab level characterization studies to establish whether any correlation existed between lab level data and SMT reflow soldering performance quantified by post-reflow solder joint yields.

EXPERIMENTAL DETAILS

Materials

Eight different solder paste materials were obtained from multiple solder paste suppliers. All solder pastes contained the SAC305 alloy with Type 4 solder powder. The main difference among the tested solder pastes was their flux chemistry. The flux in solder paste has a complex composition, normally consisting of rosin/resin, solvent, activator, and some rheological additives [3, 4]. When the temperature increases in the reflow process, the solvent in the flux starts evaporating while the activator removes the oxide on the solder and dissolves the OSP on the pads. The rosin/resin softens and liquefies to promote wetting of the molten solders on the pad surface and form the solder joint [56].

Some of the solder pastes had fluxes which contained halogenated compounds, some contained a very low amount of halogens and met the International Electrochemical Commission's (IEC) Definition of Halogen-Free, and some had zero halogens. Halogens in solder paste flux are expected to improve paste activity. The level of halogen content in the 8 solder pastes evaluated in this study are listed in Table 1.

All 8 pastes were tested for their solder bridging risk. Limited resources restricted the NWO and HoP hammer test studies to 6 and 5 pastes, respectively.

Table 1: Eight different solder pastes with different levels of halogen content were used in this study

Paste material	Halogen classification
A	Zero halogen
B	Zero halogen
C	Zero halogen
D	Halogen Free
E	Halogen Free
F	Halogen Free
G	Halogenated
H	Halogenated

NWO Hammer Test

The NWO hammer test condition was created by reducing paste volume through stencil aperture design. This led to low flux volume availability for cleaning the OSP and the oxide on the PCB pad surface leading to NWO defects. The FCBGA package substrates were 42x28 mm in size with 0.65 mm ball pitch, and these were placed on a 0.8 mm thick PCB. A special stencil with smaller-than-normal apertures was designed to increase the incidences of NWO defects. Packages were selected to have the same warpage range for all of the studies in order to reduce the impact from warpage as a variable on the results. SMT reflow was performed in air with peak temperature at 245˚C. Three legs with 12 packages per paste were run using the same conditions to ensure repeatability. Pin level paste volume data was monitored and normalized to mitigate the impact of print variance. Pin level failure rate was measured through the Dye-n-Pry failure analysis (FA) process.

HoP Hammer Test

FCBGA packages with a 42x24 mm size package, a 0.65mm ball pitch, and a 0.8 mm-thick board were used for the HoP hammer test. To create the hammer condition, the packages were baked at 125°C for 48 hours. This ensured formation of thick oxide on the solder ball surface. Additionally, a thinner stencil with a smaller aperture was designed to deposit a low paste volume with a short print height. This was done to create a deficiency of flux to clean oxide on the BGA surface. Packages were selected to have the same warpage range for all of the studies in order to reduce the impact of this variable. SMT reflow was performed in air with a peak temperature of 245˚C. The test was run twice in order to ensure repeatability with 16 packages per paste. Pin level paste volume data was monitored and normalized to mitigate the impact of variability in the printing process. HoP defect analysis was performed using a Dye-n-Pry FA process where pin level failure rate was measured for each paste.

SB Hammer Test

Solder bridging typically occurs when the solder joints compress during SMT reflow while the solder is still in the molten state. A special fixture was used to create a hammer condition to create a higher incidence of bridging defects. This fixture, as shown in Figure 5 (a), used weights (30g) to compress the center of the package during reflow. The fixture itself weighed 5g resulting in ~ 35g force on the top of each package. The packages were 20.5x16.5 mm sized BGA packages with 0.4mm ball pitch on a 0.7 mm thick PCB. Packages were selected to have the same warpage range for all of the studies in order to reduce the impact from this variable. The SMT reflow was performed in an N_2 environment with a peak temperature of 245˚C. The data was collected over multiple builds with 12 packages per paste per build. Pin level paste volume data was monitored and normalized to mitigate the impact of variability in the printing process. Bridging defect rate was determined through X-ray analysis, as shown in the Figure 5 (b).

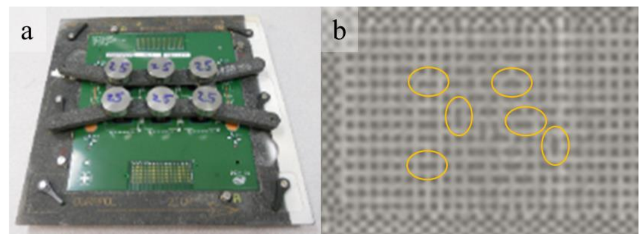

Figure 5: (a) Hammer test setup fixture with weights to compress in the middle of the package to force solder bridging during SMT reflow (b) A few of the bridging defects have been highlighted in a typical X-ray image in the center of the package post SMT.

CuOSP Solder Spread

In order to study activity of the flux, a solder spread test was performed. The test involved manual printing of paste on a CuOSP coupon using a stencil having 3 different 1.5 mm diameter aperture openings in a 0.25 mm foil thickness. Each solder paste was printed on 2 separate CuOSP coupons which provided a total of 6 solder spread data sets per paste. The reflow was performed in a small lab scale 5 zone oven. The reflow profile details are listed in Table 2.

Table 2: Profile details for the CuOSP spread testing in a lab scale reflow oven

Zone	Time (min:sec)	Temp (ºC)
1	0:45	145
2	0:45	165
3	0:45	210
4	2:15	245
5	2:15	Cool Zone

Solder spread, as well as flux spread, on CuOSP was measured under a microscope. Two readings per solder spread were taken for both solder diameter and flux spread diameter as shown in the Figure 6.

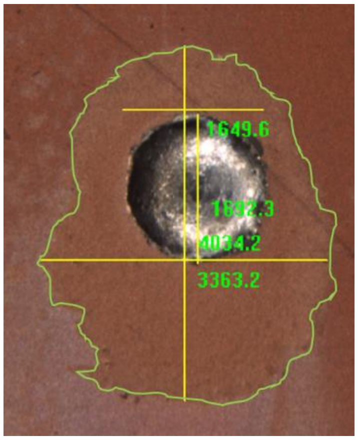

Figure 6: Representative image of the CuOSP solder spread test showing solder spread and flux spread (green outline) measurements using maximum spread diameters perpendicular to each other

Viscosity

Solder paste viscosity was measured using a Stresstech Rheometer with 40 mm plates at a 0.5 mm gap. A dynamic temperature ramp scan was performed to measure viscosity as a function of temperature from room temperature to 90˚C with a ramp rate of 3.5˚C/min.

Tackiness

Solder paste tackiness was measured at room temperature and at 50˚C using a Malcom TK-1 tackiness tester with a 5.1 mm diameter probe. The paste was printed using a 0.25 mm stencil on a frosted glass placed and heated on a hot plate. Tackiness was measured with 5 second press time, 300 g preload and a 2.5 mm/second crosshead speed according to IPC standard [7].

Thixotropic index

A shear rate sweep was performed on the solder pastes to measure viscosities at different shear rates ranging from 0.1/s to 5/s at 25ºC on AR-G2 rheometer. The thixotropic index was calculated by taking viscosity ratios at shear rates of 0.13/s and 1.3/s.

RESULTS AND DISCUSSION

NWO

The NWO defect rate was calculated at pin level based on Dye-n-Pry process using Equation (1).

$$NWO\ Rate = \frac{No.of\ solder\ joints\ with\ NWO}{Total\ no.of\ solder\ joints} \times 100 \qquad (1)$$

A significant difference was observed in the NWO defect rate between the different pastes. The NWO rate varied from 0.2% to 33% for different pastes. There was no correlation observed between halogen content of the paste and the NWO defect rate. However, a strong correlation was observed between CuOSP solder spread and the NWO rate, as shown in the Figure 7. If the flux from the paste can easily clean the OSP on the coupon surface, it will lead to a large diameter solder spread. To avoid NWO defects, the flux needs to perform its fluxing action by dissolving the OSP and reducing the copper oxides from the PCB pad surface before the solder paste lifts off the pad to ensure that there is more adhesion of the paste to the PCB pad rather than the BGA solder ball.

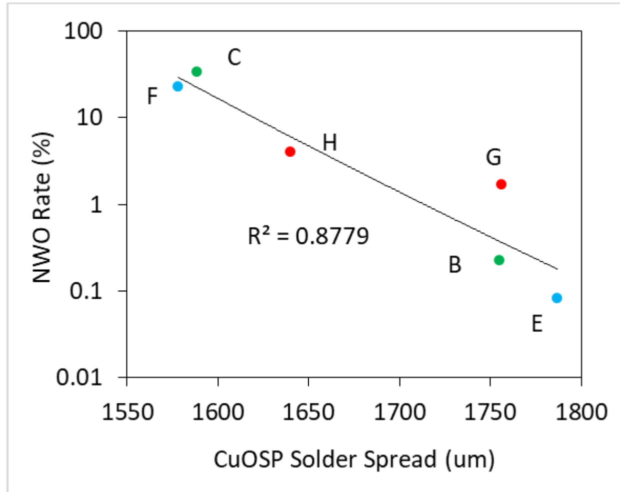

Figure 7: Plot of the Pin level NWO rate (on a log scale) and CuOSP solder spread. A logarithmic correlation is observed. Red, blue and green colors represent halogenated, halogen free compliant and zero halogen pastes respectively.

As shown in Figure 8, a couple of the solder pastes tested, C and F, had the highest NWO defect rate, and also had largest drop in tackiness as predicted by Amir et al [1]. Paste E and B with ~ 25% and 15% drop, respectively, were the best performing pastes for NWO defects. Pastes G and H were had lowest amount of drop in the tackiness, however, showed NWO defects at higher level than pastes G and H.

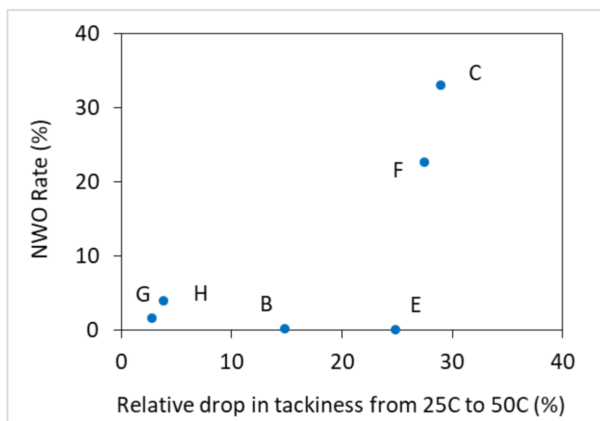

Figure 8: Drop in tackiness showed a mild correlation with NWO rate with the 2 worst performing pastes showing the largest relative drops in tack force from room temperature to high temperature.

HoP

Similar to NWO, HoP rate was also calculated at the pin level based on a Dye-n-Pry process using Equation (2).

$$HoP\ Rate = \frac{No.of\ solder\ joints\ with\ HoP}{Total\ no.of\ solder\ joints} \times 100 \quad (2)$$

Overall HoP rate varied from 0.2% to 2.8% as shown in Figure 9. Here, a negative correlation was observed between the CuOSP solder spread and the HoP resistance of the paste. This points to a potential mechanism where the active components of the flux get consumed to clean the OSP on the pad surface and cannot clean the oxide on the BGA surface.

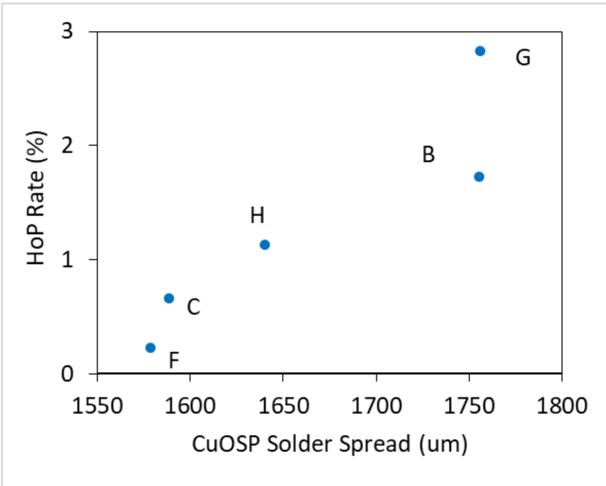

Figure 9: Pin level HoP defect rate showed inverse correlation with the CuOSP solder spread

Solder Bridging

Board to board warpage variation is small and was ignored. However, due to the variability inherent in the paste printing process, the actual paste volumes delivered to the PCB pads varied for each package. Figure 10 shows the impact of print volumes on SB defects. Paste B volume had a significant impact on the SBs. The impact made it difficult to evaluate paste performance by comparing the absolute numbers of SBs without considering the paste volume. High incidences of SB defects may have resulted from the excessive paste volume instead of the different properties of pastes.

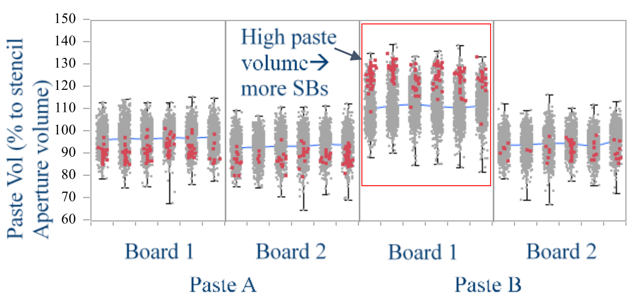

Figure 10. The variability chart of Paste Volume% for two different pastes on two different boards. Red dots represent paste volume for pins with bridging defects. Others are no bridging pins.

In order to account for this discrepancy, a weighted method is developed to mitigate the impact from paste volume so that the pastes performances can be compared. Paste volume information in terms of the percent to the aperture volume is measured by a paste inspection tool. In the weighted method, the percent paste volume is normalized to the range of (0,1) by Equation (3), where *Norm_PasteVol* is the normalized percent paste volume, Pin_{perVol} is the paste percent volume for each pin, and the $Min_{PinperVol}$ and $Max_{PinperVol}$ is the minimum and maximum percent paste volume. The weight for each SB pin, *Wgted_PasteVol*, is calculated by Equation (4), which is the inverse of the normalized paste volume. A higher paste volume will have a lower paste weight. The sum of the *Wgted_PasteVol* for all SB pins in one package is used as the weighted SB (*Weighted_SB_Risk* in Equation (5)) metric for the package.

$$Norm\_PasteVol = \frac{Pin_{PerVol} - Min_{PinperVol}}{Max_{PinperVol} - Min_{PinperVol}} \quad (3)$$

$$Wgted_{PasteVol} = \frac{1}{Norm_{PasteVol}} \quad (4)$$

$$Weighted\ SB\ Risk = Sum\left(\begin{matrix} Wgted_{PasteVol}\ for\ all\ SBed\ Pins\ of \\ a\ package \end{matrix}\right) \quad (5)$$

Figure 11 illustrates the results from the weighted SB risk and its correlation with the viscosity of the paste at high temperature (90˚C). This indicates that once the paste viscosity drops below ~ 15 Pa-s at 90˚C, the SB risk during SMT reflow increases significantly.

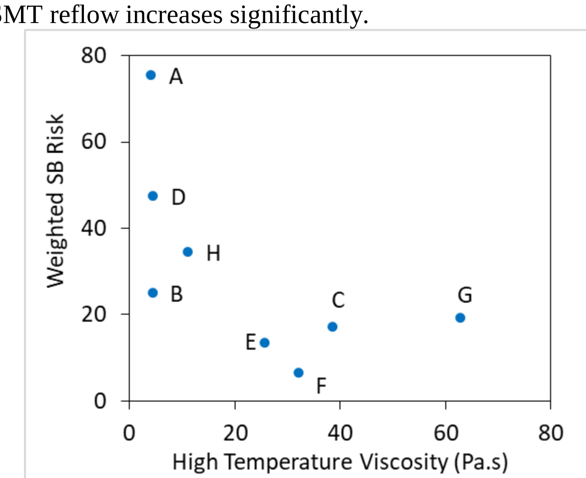

Figure 11: Plot of the High Temperature Viscosity vs the Weighted Solder Bridging Risk for all 8 solder pastes evaluated.

A similar weighted risk approach for HoP and NWO defects was explored. However, as the CuOSP solder spread test also involves paste printing, weighted approach results would be confounded by paste printing volumes for the lab level testing. Surprisingly, the weighted risk approach did not affect the HoP and NWO correlation results significantly.

Hot slump [8] under higher temperature ranges from 180°C to 205°C, for example, were evaluated as well. No correlation was observed between the hot slump and SB hammer results of the pastes.

Printability
Consistent print performance is a key aspect of a solder paste since this will significantly affect the solder joint yield and quality post SMT reflow. Therefore, a printability study was performed for the NWO SMT hammer test. The stencil aperture area ratio for this particular test was 0.60 which is more aggressive than the industry standard 0.66 for typical T4 SMT pastes. Process capability (C_p) for the paste printing showed a good correlation with the thixotropic index of the pastes, as shown in the Figure 12. A higher thixotropic index led to a higher C_p i.e. better print efficiency. As thixotropic index is ratio of low shear rate viscosity to high shear rate viscosity, higher thixotropic index indicates shear thinning or a relatively higher viscosity drop at high shear rates. This would mean relatively lower viscosity of the solder paste during shearing of the paste with squeegee to ensure maximum paste transfer into the stencil apertures. Once the paste is transferred, the relatively low viscosity at high shear rate would also help during stencil release which shears the paste ensuring better transfer of the paste on the board, and less sticking to the stencil.

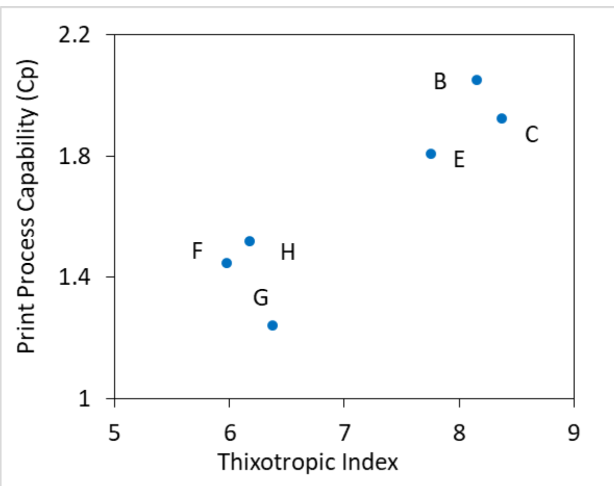

Figure 12: Plot of the Thixotropic Index vs the Print Process Capability (Cp). For all 8 solder pastes evaluated.

CONCLUSIONS
Package warpage-driven solder joint defects can be mitigated through solder paste material design. Solder paste ability to clean surface OSP was found to affect NWO and HoP resistance of the paste. If the solder paste activity triggers early to clean the CuOSP surface, it minimizes the NWO risk through early intermetallic compound formation on the pad surface. However, this reduces activity of the paste for further solder oxide cleaning leading to a higher risk for HoP. This aspect of the solder paste needs to be optimized to reduce both HoP and NWO defects to an acceptable level. Liu et al. [9] proposed two different methods viz. "tiny dot paste" and "ball onto paste" to assess HoP resistance of a paste. Scalzo [10] proposed a graping test to study heat resistance of the paste. We believe that additional tests can be used to assess the HoP / NWO risk of solder pastes. Drop in tackiness as predicted by Amir et al. [1] did not show as strong a correlation with NWO performance of the pastes as the CuOSP solder spread. Bridging defect rate for multiple pastes was observed to correlate well with high temperature viscosity. Once the viscosity drops, the flux from the paste can easily flow causing wet bridging. This eventually provides a path for molten solder to migrate from one PCB pad to its adjacent pad during reflow, thereby increasing SB risk. A high thixotropic index was observed to predict good print performance of solder pastes.

Overall, there was no correlation observed between the halogen content classification of the solder pastes and their risk of forming either NWO or HoP defects. This indicates that rosins, acids and amines in the paste have higher impact on the activity than halogen content.

The learnings from this study will be used for next generation solder paste l development at different paste suppliers. These can also be used at board assembly manufacturers (OEMs / ODMs) to assess risk level for different pastes for different defect types and as a quality check for different lots of a material.

Acknowledgement: Authors would like to thank Dr. Jinlin Wang and Peter Mckenna for support with the lab level characterizations. Authors also thank Dr. Raiyo Aspandiar for help with editing the manuscript.

REFERENCES

1. Amir, Dudi, Satyajit Walwadkar, Srinivasa Aravamudhan, and Lilia May. "The Challenges of Non Wet Open BGA Solder Defect." Proceedings of SMTA International Conference. 2012.
2. Amir, Dudi, Raiyo Aspandiar, Scott Buttars, Wei Chin, and Paramjeet Gill. "Head–and–Pillow SMT Failure Modes." Proceedings of the SMTA International Conference, (2009, pp 409-421.
3. Indium, "Understanding flux vehicle chemistry," Available online: documents.indium.com/qdynamo/download.php?docid=296
4. Lentz, Tony, and F. C. T. Assembly. "Dispelling the Black Magic of Solder Paste." Proceedings of the IPC Apex Expo Conference, 2015.
5. D. Baluch and G. Minogue, "Fundamentals of solder paste technology," Global SMT & Packaging, Dec. 2017. Available online: https://www.smtnet.com/library/files/upload/fundamentals_of_solder_paste_technology.pdf
6. Itoh, M. General information on solder paste. Technical Report, KOKI Company Limited, Tokyo, Japan, 1999.
7. IPC-TM-650, version 2.4.44 "Solder Paste—Tack Test" Available online: https://www.ipc.org/TM/2.4.44.pdf
8. IPC-TM-650, version 2.4.35, "Solder paste-slump test," Available online: https://www.ipc.org/TM/2.4.35.pdf
9. Liu, Yan, Pamela Fiacco, and Ning-Cheng Lee. "Testing and prevention of head-in-pillow." Proceeding of the

Electronic Components and Technology Conference (ECTC), IEEE, 2010 pp. 451-455.
10. Bath, Jasbir, Roberto Garcia, Noriyoshi Uchida, Hajime Takahashi, Gordon Clark, and Manabu Itoh. "Investigation and development of tin-lead and lead-free solder pastes to reduce the head-in-pillow component soldering defect." Global SMT & Packaging, Vol 9, no. 12 (2009): 10-16.